

Supporting information to:

Determinants of Regioselectivity and Chemoselectivity in Fosfomycin Resistance Protein FosA from QM/MM Calculations

Rong-Zhen Liao, Walter Thiel*

*Max-Planck-Institut für Kohlenforschung, Kaiser-Wilhelm-Platz 1, D-45470,
Mülheim an der Ruhr, Germany*

*Corresponding Author: thiel@kofo.mpg.de

Contents:

1.	System preparation using CHARMM version C31B1	S2
2.	QM calculations of the uncatalyzed reaction	S7
3.	Enzymatic GSH addition	S13
4.	Enzymatic water addition	S22
5.	Complete citations for references 42, 53, and 55	S28

1. System preparation using CHARMM version C31B1

1.1 Preparation of the PDB structure.

The dimeric form of FosA (PDB code: 1LQP, resolution 1.19 Å) was used for preparing the system. The orientations of Asn, Gln, and His side chains were adjusted manually according to their local hydrogen-bonding network when necessary. The flipped residues are listed below:

His: 107, both chain A and B.

The active region included all atoms within 30 Å of the manganese atom of chain A. All Lys and Arg residues were chosen to be protonated at their side chains and all Glu and Asp residues were deprotonated at their side chains. All Tyr residues were chosen to be protonated at their side chains except Tyr39 of chain A (the catalytic base). The protonation states of His residues were chosen as follows:

HSD (proton at ND1): 7, 64, 84, 112, both chain A and B

HSP (protons at both ND1 and NE2): 107, both chain A and B

1.2 CHARMM parameters.

Parameters for fosfomycin are specified below (CHELPG charges were calculated at the B3LYP/def2-SVP level).

```
RESI FCN      -2.000 !
ATOM C1       CT1      -0.02 !
ATOM H1       HA       -0.01 !
ATOM C2       CT1      0.21 !
ATOM H2       HA       -0.08 !
ATOM C3       CT3      -0.09 !          O2P   H1   H2   H4
ATOM O1       OS       -0.49 !          |     |     |     |
ATOM P        P        1.36 !          O1P--P---C1---C2---C3--H3
ATOM O1P      ON3      -0.97 !          |     \   /   |
ATOM O2P      ON3      -0.97 !          O3P     O1     H5
ATOM O3P      ON3      -0.97 !
ATOM H3       HA       0.01 !
ATOM H4       HA       0.01 !
ATOM H5       HA       0.01 !
BOND C1     P     C1   O1    C1   H1
BOND P      O1P    P    O2P   P O3P
BOND C2     O1    C2   H2
BOND C3     C2    C3   H4    C3   H5    C3   H3
PATCHING FIRST NONE LAST NONE
```

Notice: The topology files for fosfomycin were only used for the setup of QM/MM calculations. We do not recommend using them for classical MM calculations without extensive validation.

1.3 System hydration.

The system with added hydrogen atoms was hydrated using a water droplet composed of a 40 Å sphere of equilibrated TIP3 water molecules centered at manganese of chain A. All water molecules with their oxygen atoms within 2.8 Å of any protein non-hydrogen atom were deleted. Following this, the water sphere and the GSH substrate was subjected to energy minimization [steepest descent (SD) for 1000 steps and adapted-basis Newton Raphson (ABNR) for 3000 steps] and to molecular dynamics (MD) for 50 ps (20 ps heating to 300K) with a stochastic boundary potential³ using the CHARMM force field implemented in the CHARMM program.⁴ During the whole procedure, all non-H atoms of non-TIP3 residues (protein, fosfomycin, Mn and its ligands) were kept fixed. The water molecules were kept rigid during the heating period using the SHAKE constraint algorithm.⁵ Finally, the water molecules and the GSH substrate were minimized for 3000 steps using the ABNR method. The final structure then served as the starting structure for subsequent solvation. This procedure was repeated five times (six solvations in total). The number of water molecules added each time is shown below:

Number of water molecules added					
Sol-1	Sol-2	Sol-3	Sol-4	Sol-5	Sol-6
6931	694	318	202	183	103

1.4 System equilibration.

Following system neutralization, the system was subjected to a 1 ns MD simulation with a 1 fs timestep. The simulation employed Langevin dynamics and a stochastic boundary potential.³ An active region was defined including all protein residues within 30 Å of the manganese ion of chain A. Within this region, the manganese ion and the non-hydrogen atoms of His7, His64, Glu110, and fosfomycin were kept fixed. The system was first minimized for 3600 ABNR steps, then heated to 300K for 20ps (with SHAKE constraints⁵), and finally equilibrated for 1 ns. Five random snapshots were used for QM/MM calculations. The quality of the structure was assessed by calculating the root-mean-square deviation (RMSD) between the Cartesian coordinates of each snapshot and the crystal structure:

	100ps	200ps	300ps	400ps	500ps	600ps	700ps	800ps	900ps	1ns
RMSD (Å)	0.744	0.797	0.826	0.812	0.850	0.813	0.854	0.826	0.909	0.896

For setting up the system for the water attack reaction, the GSH substrate was deleted, solvated with water molecules, and neutralized by adding one chloride ion. The system was then equilibrated for 1 ns using the same procedure as for the GSH system. The final snapshot was then used for QM/MM calculations.

References:

1. Sawai, H.; Sugimoto, H.; Kato, Y.; Asano, Y.; Shiro, Y.; Aono, S. *J. Biol. Chem.* **2009**, 284, 32089-32096.
2. Schnur, D. M.; Dalton, D. R. *J. Org. Chem.* **1988**, 53, 3313-3316.
3. Brooks, C. L.; Karplus, M. *J. Chem. Phys.* **1983**, 79, 6312-6325.
4. Brooks, B. R.; Brucolieri, R. E.; Olafson, B. D.; States, D. J.; Swaminathan, S.; Karplus, M. *J. Comput. Chem.* **1983**, 4, 187-217.
5. Ryckaert, J. P.; Cicotti, G.; Berendsen, H. J. C. *J. Comput. Phys.* **1977**, 23, 327-341.
6. Boucher, J.-L.; Delaforge, M.; Mansuy, D. *Biochemistry* **1994**, 33, 7811-7818.

2. QM calculations of the uncatalyzed reaction

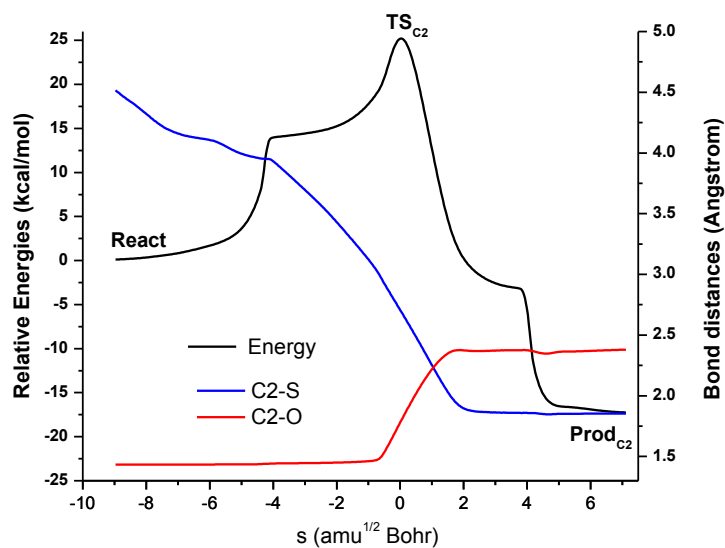
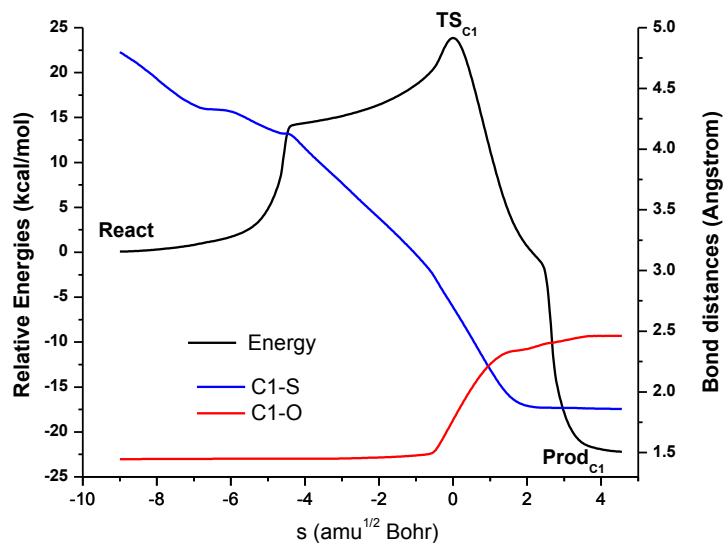


Figure S1. Changes in energy (relative to **React**) along the IRC paths for the attack at C1 (top) and C2 (bottom) with a step size of $0.03 \text{ amu}^{1/2}\text{Bohr}$.

Table S1. Calculated energies (in Hartree) of reactant, transition states, and products for the uncatalyzed reaction at various levels.

	React	TS _{C1}	TS _{C2}	Prod _{C1}	Prod _{C2}
B3LYP/def2-SVP	-1351.224283	-1351.186271	-1351.184124	-1351.259669	-1351.250377
B3LYP/def2-SVP-SMD	-1351.30458	-1351.262462	-1351.260411	-1351.348147	-1351.342446
B3LYP/def2-TZVPP	-1352.268321	-1352.226869	-1352.226065	-1352.303376	-1352.298048
M06/def2-TZVPP	-1351.863841	-1351.822648	-1351.821546	-1351.903805	-1351.894304
wB97X/def2-TZVPP	-1352.073646	-1352.023133	-1352.023077	-1352.113398	-1352.106266
B2PLYP/def2-TZVPP	-1351.557514	-1351.520002	-1351.518285	-1351.601156	-1351.593697
Free energy corrections	0.153861	0.155579	0.155187	0.161453	0.158949

React

Center Number	Atomic Number	Atomic Type	Coordinates (Angstroms)		
			X	Y	Z
1	6	0	1.057337	0.908605	1.049986
2	6	0	0.699484	2.150150	0.335416
3	6	0	0.105875	2.209015	-1.046920
4	8	0	2.073697	1.766351	0.477347
5	15	0	0.893402	-0.822382	0.419682
6	8	0	-0.278107	-1.453934	1.142114
7	8	0	2.300547	-1.457221	0.970779
8	8	0	0.932858	-0.811804	-1.117274
9	16	0	-3.553167	0.486483	-0.493114
10	6	0	-3.249131	0.143004	1.285433
11	8	0	3.576187	-0.180379	-1.134617
12	1	0	-1.364583	-2.107693	-0.310606
13	1	0	1.030005	0.946656	2.150320
14	1	0	0.440841	3.006990	0.979742
15	1	0	0.412695	1.329286	-1.627320
16	1	0	0.421010	3.134798	-1.558981
17	1	0	-0.994841	2.199140	-0.977157
18	1	0	3.003548	-1.164699	0.342818
19	1	0	-2.233244	-0.260490	1.416172
20	1	0	-3.348220	1.087138	1.842186
21	1	0	-3.981130	-0.577714	1.683699
22	1	0	2.692621	-0.485107	-1.457810
23	1	0	3.316573	0.663906	-0.721864
24	8	0	-1.613749	-2.050346	-1.258930
25	1	0	-0.786116	-1.637760	-1.585486
26	1	0	-2.772356	-0.548440	-0.959964

TS_{C1}

Center Number	Atomic Number	Atomic Type	Coordinates (Angstroms)		
			X	Y	Z
1	6	0	-0.200187	0.793657	-0.728243
2	6	0	-0.788450	1.982200	-0.108307
3	6	0	-0.961352	2.131304	1.390388
4	8	0	-1.844680	1.431628	-0.853565
5	15	0	-0.487449	-0.934446	-0.212137
6	8	0	0.765817	-1.816370	-0.659949
7	8	0	-1.604684	-1.504873	-1.221165
8	8	0	-0.866091	-1.049075	1.247846
9	16	0	2.321477	1.025741	0.202835
10	6	0	3.258418	0.407248	-1.246409
11	8	0	-3.584391	-0.341128	0.153602
12	1	0	1.381164	-1.901114	0.140025
13	1	0	0.221868	0.918975	-1.725998
14	1	0	-0.391634	2.919754	-0.545679
15	1	0	-1.234497	1.175885	1.856658
16	1	0	-1.743506	2.882611	1.595821
17	1	0	-0.016682	2.481252	1.836697
18	1	0	-2.488919	-1.170934	-0.903722
19	1	0	2.852359	-0.554243	-1.601576
20	1	0	3.218757	1.124344	-2.086256
21	1	0	4.323228	0.255926	-0.994597
22	1	0	-3.044181	-0.634653	0.909062
23	1	0	-3.081718	0.463608	-0.146463
24	8	0	2.001697	-1.709047	1.636566
25	1	0	1.102575	-1.546582	1.980875

26	1	0	2.277378	-0.785534	1.350581
----	---	---	----------	-----------	----------

TS_{C2}

Center Number	Atomic Number	Atomic Type	Coordinates (Angstroms)		
			X	Y	Z
1	6	0	-0.403864	0.711480	-0.879516
2	6	0	0.328335	1.718298	-0.111298
3	6	0	0.135146	2.032377	1.346335
4	8	0	-1.311254	1.777781	-0.837260
5	15	0	-0.971063	-0.892179	-0.160521
6	8	0	-2.308073	-1.205064	-1.008366
7	8	0	-1.184645	-0.855984	1.337678
8	8	0	0.032545	-2.023697	-0.671917
9	16	0	2.766237	0.633467	0.256836
10	6	0	3.070564	-0.034400	-1.424740
11	8	0	-3.520623	0.787163	0.305531
12	1	0	-2.988130	-0.551898	-0.680092
13	1	0	0.010970	0.487776	-1.881972
14	1	0	0.877859	2.438344	-0.715299
15	1	0	-0.298632	1.177836	1.880434
16	1	0	-0.538225	2.899846	1.451474
17	1	0	1.102449	2.293461	1.796997
18	1	0	0.727567	-2.170239	0.064344
19	1	0	2.354954	-0.832839	-1.682920
20	1	0	2.986296	0.754899	-2.193684
21	1	0	4.088117	-0.457478	-1.501965
22	1	0	-3.089051	0.403381	1.089019
23	1	0	-2.780909	1.337900	-0.078776
24	8	0	1.568046	-2.013783	1.395698
25	1	0	0.794011	-1.653608	1.867350
26	1	0	2.069814	-1.178025	1.127939

Prod_{C1}

Center Number	Atomic Number	Atomic Type	Coordinates (Angstroms)		
			X	Y	Z
1	6	0	0.188504	0.820509	-0.534912
2	6	0	-0.847006	1.828196	0.062730
3	6	0	-0.948956	1.784275	1.593537
4	8	0	-2.102782	1.720489	-0.552124
5	15	0	-0.292953	-0.994202	-0.442357
6	8	0	1.113800	-1.784611	-0.772256
7	8	0	-1.287340	-1.259854	-1.551264
8	8	0	-0.682456	-1.318797	1.013752
9	16	0	1.856168	1.208298	0.189167
10	6	0	2.940492	0.765895	-1.207984
11	8	0	-3.340483	-0.684291	0.103242
12	1	0	1.548977	-1.987788	0.091998
13	1	0	0.257519	1.045923	-1.611080
14	1	0	-0.463272	2.828435	-0.215598
15	1	0	-1.235774	0.778795	1.931427
16	1	0	-1.705365	2.516549	1.918796
17	1	0	0.011112	2.042163	2.071693
18	1	0	-2.849450	-0.990229	-0.700433
19	1	0	2.738761	-0.270602	-1.511306
20	1	0	2.784762	1.450010	-2.057563

21	1	0	3.979792	0.860252	-0.858048
22	1	0	-2.705206	-1.003573	0.775031
23	1	0	-2.566031	0.900651	-0.252036
24	8	0	1.803495	-1.816862	1.882998
25	1	0	0.812238	-1.743451	1.819199
26	1	0	2.055487	-0.888730	1.731591

Prod_{C2}

Center Number	Atomic Number	Atomic Type	Coordinates (Angstroms)		
			X	Y	Z
1	6	0	0.495571	-0.913037	-0.268945
2	6	0	-0.761885	-1.527996	0.385200
3	6	0	-0.711888	-1.511524	1.915492
4	8	0	1.559162	-1.723615	0.198574
5	15	0	0.832411	0.925202	-0.017785
6	8	0	2.262414	1.146531	-0.488034
7	8	0	0.395096	1.406680	1.366115
8	8	0	-0.179077	1.606545	-1.136338
9	16	0	-2.396403	-0.818544	-0.111522
10	6	0	-2.286967	-0.750682	-1.929385
11	8	0	4.042048	-0.697354	-0.470939
12	8	0	-1.956960	2.481419	0.758025
13	1	0	3.435075	0.103161	-0.589357
14	1	0	0.391145	-1.015694	-1.370020
15	1	0	-0.779307	-2.579578	0.046538
16	1	0	-0.646463	-0.477008	2.281443
17	1	0	0.197175	-2.041510	2.233465
18	1	0	-1.592234	-2.016662	2.346973
19	1	0	-0.900778	2.069805	-0.644033
20	1	0	-1.561091	0.015568	-2.235621
21	1	0	-2.020383	-1.734040	-2.348567
22	1	0	-3.289625	-0.474346	-2.289699
23	1	0	4.266521	-0.611593	0.466400
24	1	0	2.421777	-1.397997	-0.148154
25	1	0	-1.096700	2.236559	1.201789
26	1	0	-2.359276	1.599801	0.666592

3. Enzymatic GSH addition

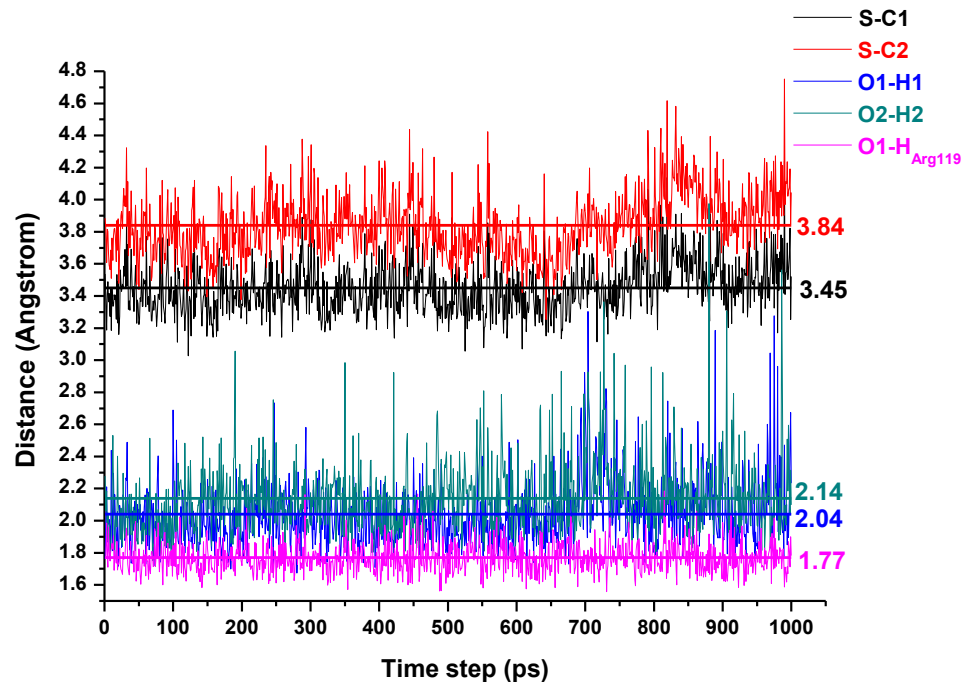


Figure S2. Evolution of selected distances in Å during the MD simulation. The average value is also indicated. The atom labels are defined in **Figure 3**.

For Sn1, the following residues (within 13 Å of C1 of fosfomycin, 1383 atoms) were allowed to move during the geometry optimizations:

Chain A: LEU5, ASN6, HSD7, LEU8, THR9, LEU10, ALA11, VAL12, LEU15, GLU31, ALA32, ARG33, TRP34, GLN36, GLY37, ALA38, TYN39, LEU40, GLU41, LEU45, TRP46, LEU47, CYS48, LEU49, SER50, ARG51, GLU52

Chain B: ASP61, TYR62, THR63, HSD64, TYR65, ALA66, PHE67, GLY68, PHE74, TRP89, LYS90, GLN91, ASN92, ARG93, SER94, GLU95, GLY96, ASP97, SER98, PHE99, TYR100, PHE101, ARG108, LEU109, GLU110, ALA111, HSD112, VAL113, GLY114, ASP115, LEU116, ARG117, SER118, ARG119, LEU120, ALA122, CYS123, TYR128, MET131

Water: CRYW47, CRYW56, CRYW67, CRYW69, CRYW75, CRYW133, CRYW153, CRYW170, CRYW246, WZ116, WZ1364, WZ1378, WZ1466, WZ1693, WZ1866, WZ11081, WZ11271, WZ11334, WZ11377, WZ11435, WZ11471, WZ11599, WZ11632, WZ11661, WZ11703, WZ11863, WZ12058, WZ12116, WZ12245, WZ12323, WZ12333, WZ12374, WZ12422, WZ12524, WZ12644, WZ12725, WZ12946, WZ12959, WZ13004, WZ13061, WZ13242, WZ13243, WZ13879, WZ13889, WZ217, WZ225, WZ295, WZ2183, WZ2237, WZ2372, WZ2613, WZ2651, WZ2672, WZ2690, WZ2863, WZ21265, WZ21320, WZ21328, WZ21467, WZ21781, WZ21849, WZ21864, WZ22061, WZ22207, WZ22214, WZ22421, WZ22588, WZ22602, WZ22810, WZ23036, WZ23044, WZ23212, WZ23308, WZ23415, WZ23514, WZ23522, WZ23566, WZ23599, WZ23686, WZ23806, WZ3166, WZ3174

Mn, Fosfomycin, and GSH

3.1 QM region M1a (87 atoms) for GSH addition

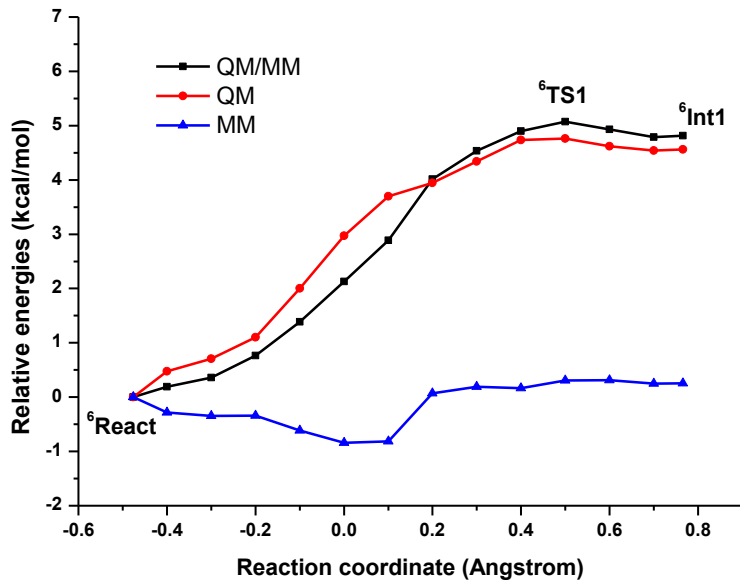


Figure S3. Energy profile for proton transfer between GSH and Tyr39 in the lowest sextet state computed at the QM(B3LYP/def2-SVP)/CHARMM level using the reaction coordinate $d_{S-H1} - d_{O1-H1}$ for QM region M1a.

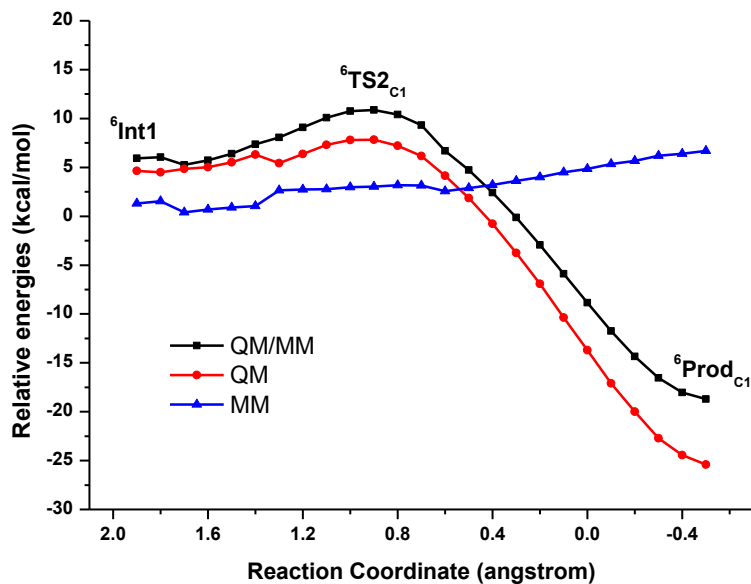


Figure S4. Energy profile for the GSH attack at C1 in the lowest sextet state computed at the QM(B3LYP/def2-SVP)/CHARMM level using the reaction coordinate $d_{S-C1} - d_{O2-C1}$ for QM region M1a.

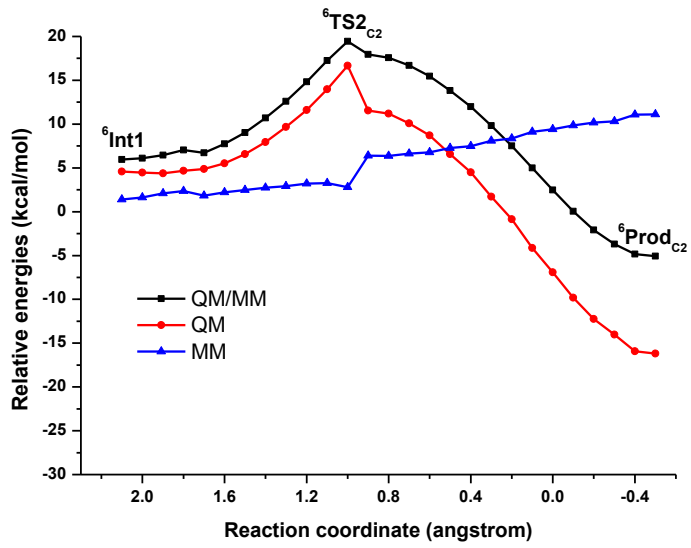


Figure S5. Energy profile for the GSH attack at C2 in the lowest sextet state computed at the QM(B3LYP/def2-SVP)/CHARMM level using the reaction coordinate $d_{S\text{-C}2} - d_{O_2\text{-C}2}$ for QM region M1a.

Table S2. Calculated QM, MM, QM/MM and dispersion energies (in Hartree) of optimized stationary points for GSH attack using QM region **M1a**.

	B3LYP/BS1:MM			B3LYP/ TZVPP:MM		Dispersion
	QM	MM	QM/MM	QM	QM/MM	
⁶ React	-3831.347634	-156.507944	-3987.855578	-3834.036635	-3990.5446	-0.123466
⁴ React	-3831.289179	-156.508194	-3987.797373	-3833.980683	-3990.4889	-0.125599
² React	-3831.263952	-156.507940	-3987.771892	-3833.956886	-3990.4648	-0.126501
⁶ TS1	-3831.339885	-156.507689	-3987.847574	-3834.028638	-3990.5363	-0.122160
⁶ Int1	-3831.340365	-156.507543	-3987.847908	-3834.029821	-3990.5356	-0.121632
⁶ TS2_{C1}	-3831.335269	-156.502985	-3987.838254	-3834.021428	-3990.5244	-0.125852
⁶ TS2_{C2}	-3831.328819	-156.498103	-3987.826922	-3834.015748	-3990.5139	-0.125399
⁶ Prod_{C1}	-3831.388277	-156.497221	-3987.885498	-3834.073004	-3990.5702	-0.128134
⁶ Prod_{C2}	-3831.373564	-156.490236	-3987.863800	-3834.057379	-3990.5476	-0.128347

3.2 QM region M2a (170 atoms) for GSH addition

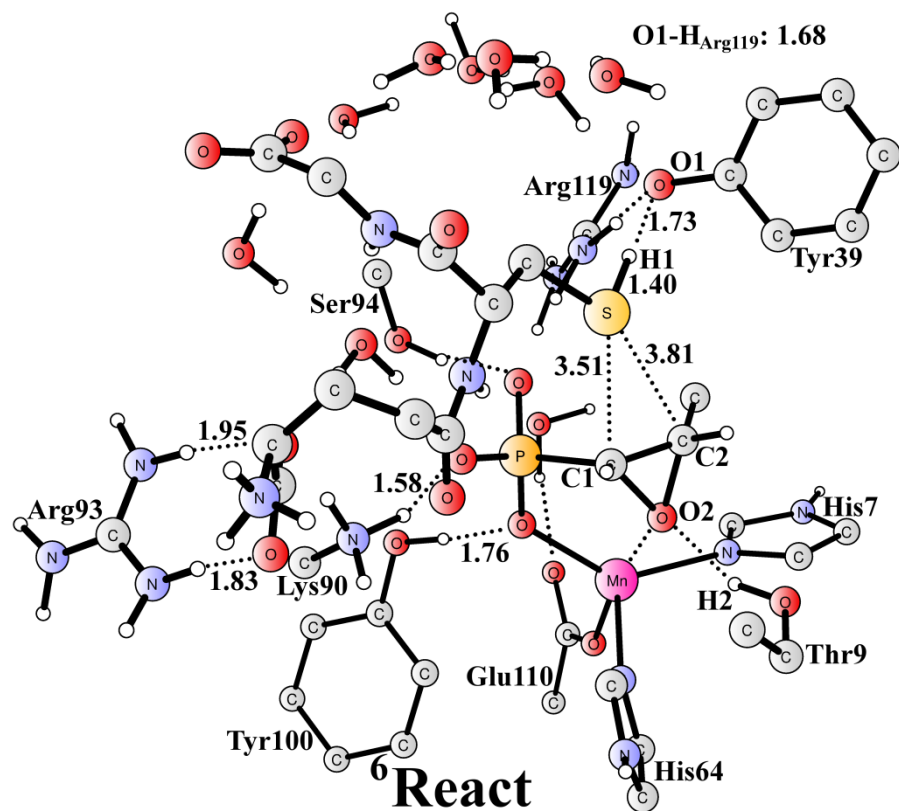


Figure S6. Optimized structure of reactant complex (⁶React) for QM region M2a (B3LYP/MM). For clarity, unimportant hydrogen atoms are not shown. Distances are given in Å.

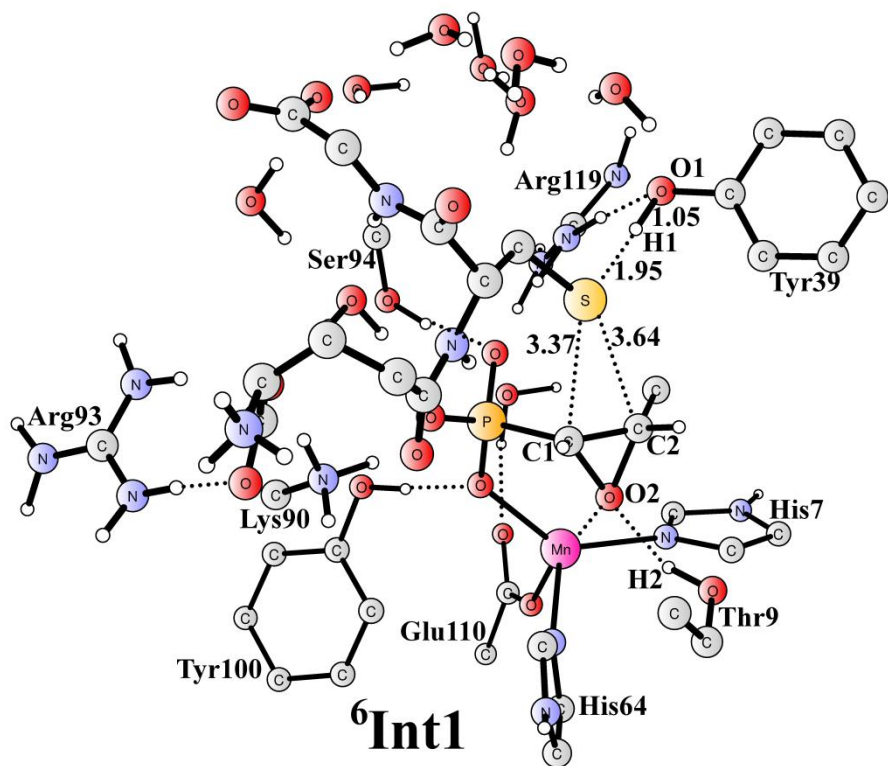
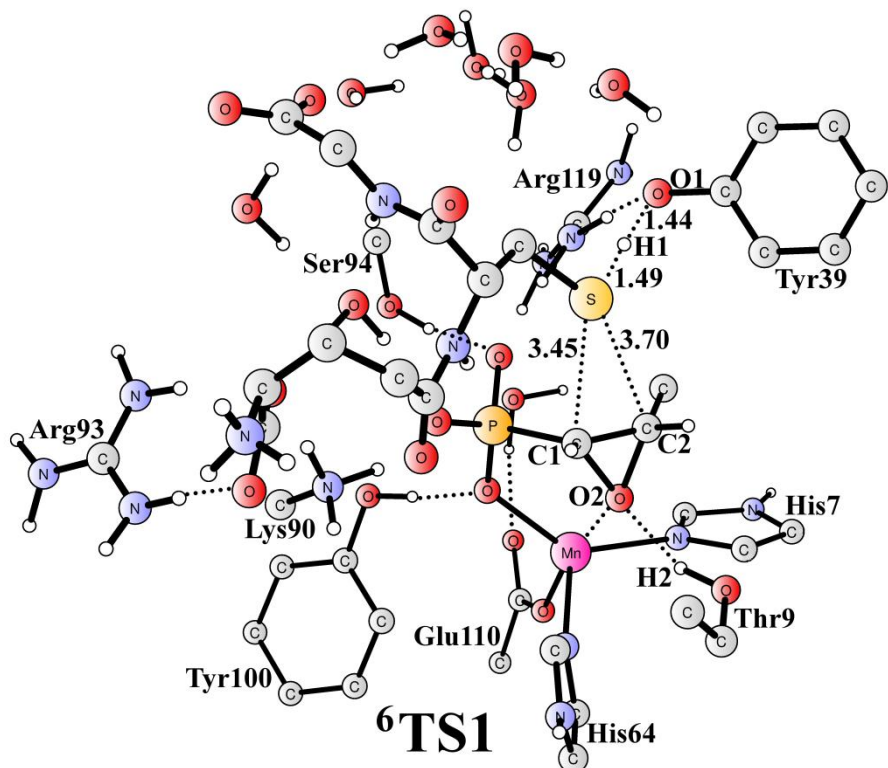


Figure S7. Optimized structure of transition state (⁶TS1) and intermediate (⁶Int1) for proton transfer for GSH attack with QM region M2a (B3LYP/MM). For clarity, unimportant hydrogen atoms are not shown. Distances are given in Å.

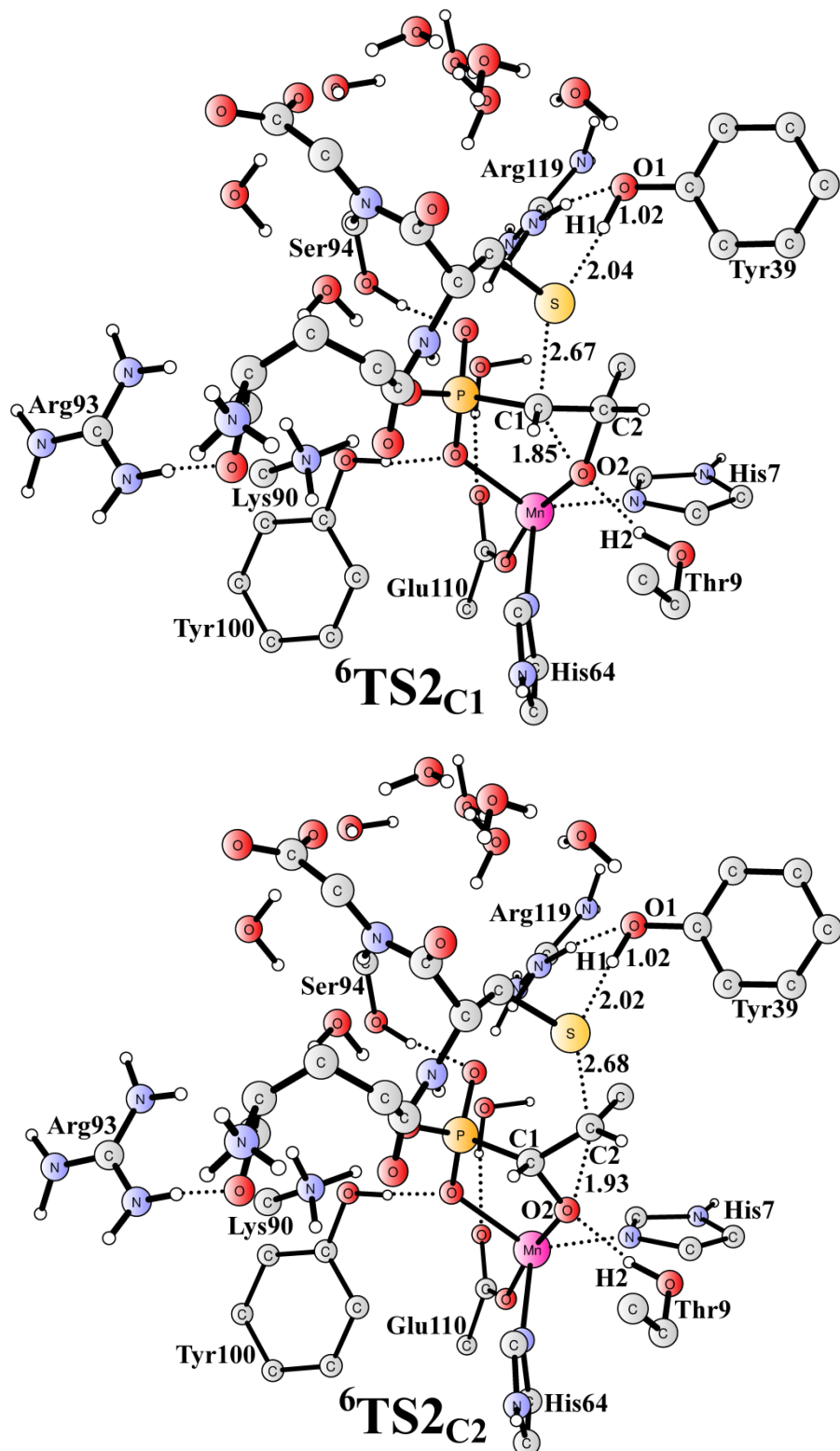


Figure S8. Optimized structure of transition states for the attack on C1 (${}^6\text{TS2}_{\text{C}1}$) and C2 (${}^6\text{TS2}_{\text{C}2}$) for GSH attack with QM region M2a (B3LYP/MM). For clarity, unimportant hydrogen atoms are not shown. Distances are given in Å.

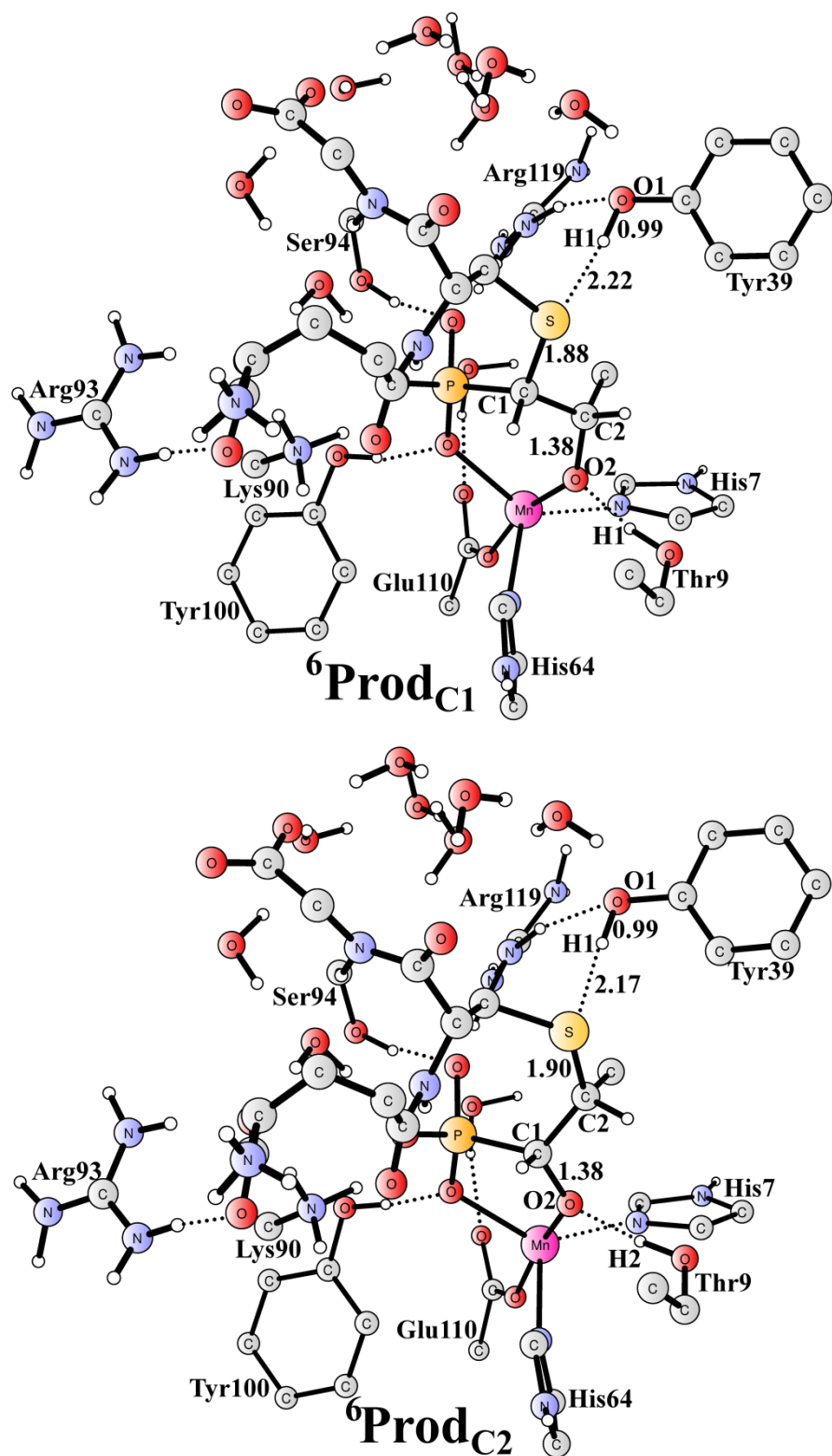


Figure S9. Optimized structure of product complexes for the attack on C1 (${}^6\text{Prod}_{\text{C}1}$) and C2 (${}^6\text{Prod}_{\text{C}2}$) for GSH attack with QM region M2a (B3LYP/MM). For clarity, unimportant hydrogen atoms are not shown. Distances are given in Å.

Table S3. Calculated QM, MM, QM/MM and dispersion energies (in Hartree) of optimized stationary points for GSH attack using QM region **M2a**.

	B3LYP/BS1:MM			B3LYP/ TZVPP:MM		Dispersion
	QM	MM	QM/MM	QM	QM/MM	
⁶ React	-6072.603482	-155.221188	-6227.824670	-6077.958242	-6233.179430	-0.289562
⁴ React	-6072.545688	-155.222055	-6227.767743	-6077.902712	-6233.124767	-0.292053
² React	-6072.520505	-155.222191	-6227.742696	-6077.878308	-6233.100499	-0.293156
⁶ TS1	-6072.596297	-155.223800	-6227.820097	-6077.947486	-6233.171286	-0.292667
⁶ Int1	-6072.602013	-155.222549	-6227.824562	-6077.954512	-6233.177061	-0.292130
⁶ TS2_{C1}	-6072.586467	-155.223237	-6227.809704	-6077.934824	-6233.158061	-0.296474
⁶ TS2_{C2}	-6072.577932	-155.219054	-6227.796986	-6077.927126	-6233.146180	-0.294173
⁶ Prod_{C1}	-6072.623224	-155.222922	-6227.846146	-6077.967225	-6233.190147	-0.300019
⁶ Prod_{C2}	-6072.606502	-155.221691	-6227.828193	-6077.946019	-6233.167710	-0.301518

4. Enzymatic water Addition

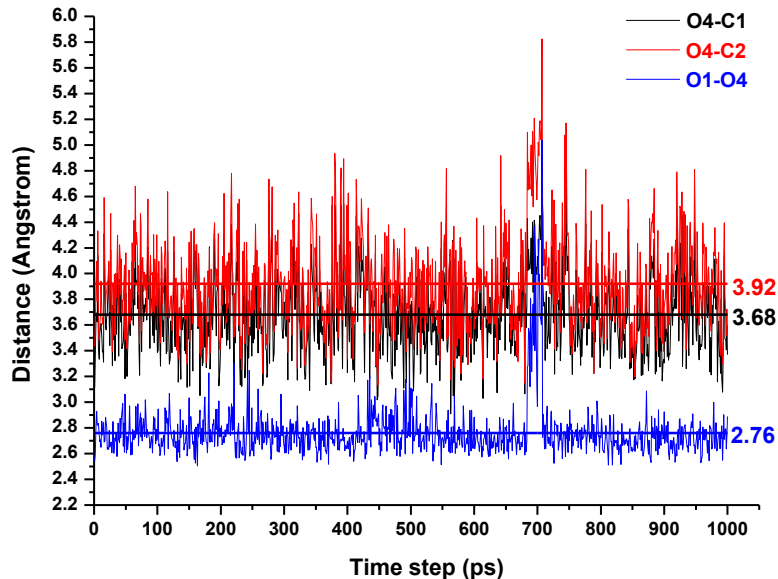


Figure S10. Evolution of selected distances in Å during the MD simulation. The average value is also indicated. The atom labels are defined in **Figure 8**.

The following residues (within 13 Å of C1 of fosfomycin, 1383 atoms) were allowed to move during the geometry optimizations:

Chain A: LEU5, ASN6, HSD7, LEU8, THR9, LEU10, ALA11, VAL12, LEU15, GLU31, ALA32, ARG33, TRP34, GLN36, GLY37, ALA38, TYN39, LEU40, LEU45, TRP46, LEU47, CYS48, LEU49, SER50, ARG51, GLU52, PRO53

Chain B: ASP61, TYR62, THR63, HSD64, TYR65, ALA66, PHE67, TRP89, LYS90, GLN91, ASN92, ARG93, SER94, GLU95, GLY96, ASP97, SER98, PHE99, TYR100, PHE101, ARG108, LEU109, GLU110, ALA111, HSD112, VAL113, GLY114, ASP115, LEU116, SER118, ARG119, LEU120, ALA122, CYS123, TYR128, MET131

Water: CRYW47, CRYW56, CRYW67, CRYW153, CRYW170, CRYW283, CRYW365, WZ118, WZ1120, WZ1558, WZ1622, WZ1696, WZ1772, WZ1949, WZ11209, WZ11223, WZ11237, WZ11333, WZ11372, WZ11414, WZ11510, WZ11525, WZ11533, WZ11609, WZ11708, WZ11780, WZ11856, WZ11882, WZ11909, WZ11996, WZ12021, WZ12100, WZ12331, WZ12374, WZ12642, WZ12669, WZ12693, WZ12732, WZ12847, WZ13002, WZ13073, WZ13255, WZ13335, WZ13408, WZ13421, WZ13495, WZ13637, WZ13719, WZ13746, WZ13755, WZ13943, WZ25, WZ223, WZ2130, WZ2164, WZ2238, WZ2445, WZ2468, WZ2670, WZ2687, WZ2738, WZ2951, WZ21232, WZ21311, WZ21381, WZ21382, WZ21474, WZ21531, WZ21598, WZ21621, WZ21726, WZ21951, WZ22017, WZ22173, WZ22250, WZ22382, WZ22400, WZ22519, WZ22548, WZ22592, WZ22775, WZ22821, WZ22845, WZ22891, WZ22936, WZ23149, WZ23184, WZ23192, WZ23209, WZ23321, WZ23508, WZ23715, WZ23739, WZ23800, WZ23960, WZ314, WZ3181, WZ3227, WZ3415, WZ3451, WZ3452, WZ3471, WZ3475, WZ3477,

Mn and Fosfomycin

4.1 QM region M1b (81 atoms) for water addition

Table S4. Calculated QM, MM, QM/MM and dispersion energies (in Hartree) of optimized stationary points for water attack using QM region **M1b**.

	B3LYP/BS1:MM			B3LYP/ TZVPP:MM		Dispersion
	QM	MM	QM/MM	QM	QM/MM	
⁶ React	-3429.987987	-157.134642	-3587.122629	-3432.550755	-3589.685397	-0.113163
⁴ React	-3429.931346	-157.133351	-3587.064697	-3432.495226	-3589.628577	-0.116192
² React	-3429.904767	-157.133511	-3587.038278	-3432.470154	-3589.603665	-0.116976
⁶ TS2_{C1}	-3429.959221	-157.132571	-3587.091792	-3432.517072	-3589.648954	-0.117253
⁶ TS2_{C2}	-3429.961360	-157.135015	-3587.096375	-3432.520149	-3589.655164	-0.116147
⁶ Prod_{C1}	-3429.995791	-157.135332	-3587.131123	-3432.549422	-3589.684754	-0.116119
⁶ Prod_{C2}	-3430.004464	-157.135835	-3587.140299	-3432.554878	-3589.690713	-0.116017

4.2 QM region M2b (170 atoms) for water addition

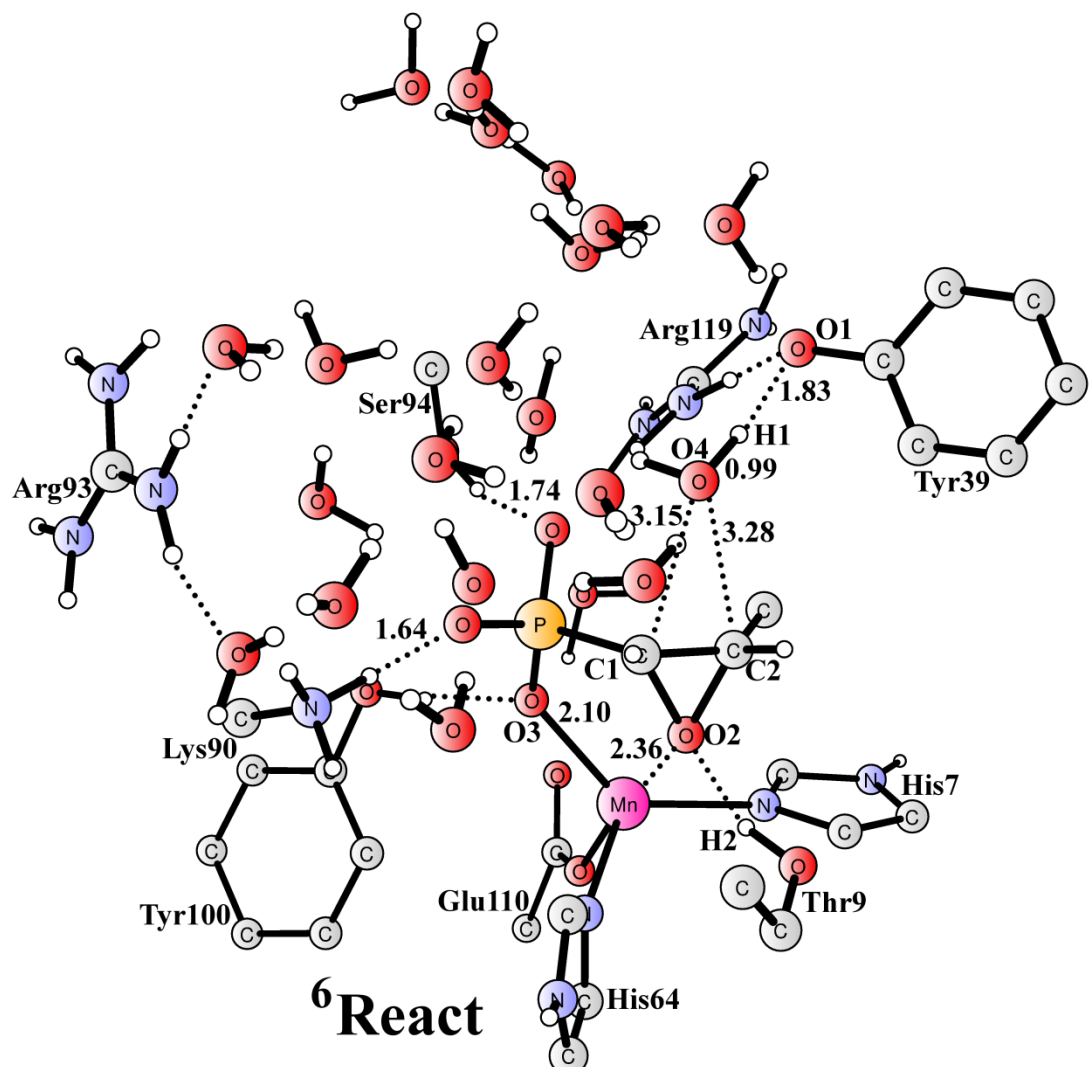


Figure S11. Optimized structure of reactant complex (**React**) for water attack with QM region M2b (B3LYP/MM). For clarity, unimportant hydrogen atoms are not shown. Distances are given in Å.

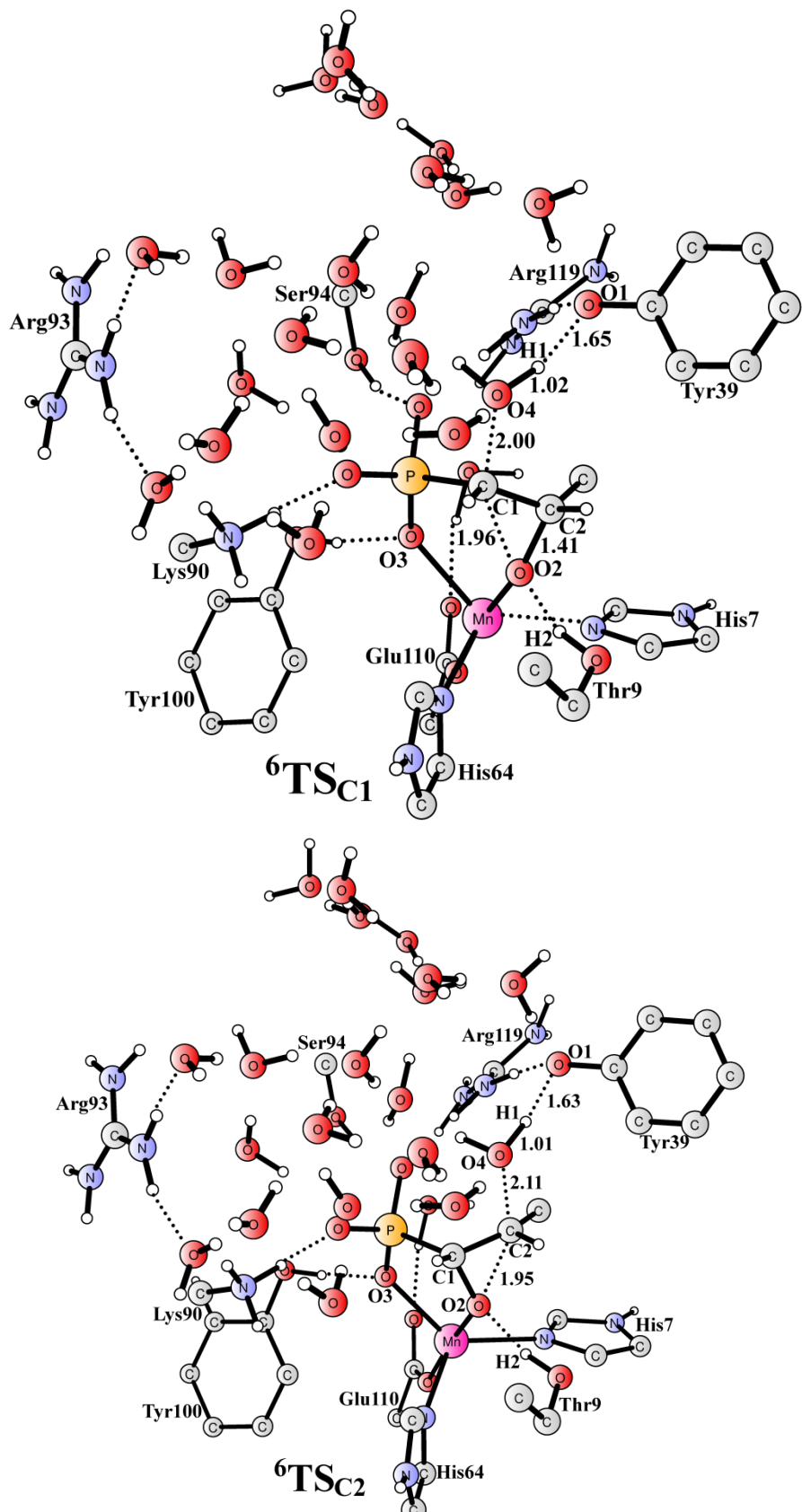


Figure S12. Optimized structure of transition states for the attack on C1 (${}^6\text{TS}_{\text{C}1}$) and C2 (${}^6\text{TS}_{\text{C}2}$) for water attack with QM region M2b (B3LYP/MM). For clarity, unimportant hydrogen atoms are not shown. Distances are given in Å.

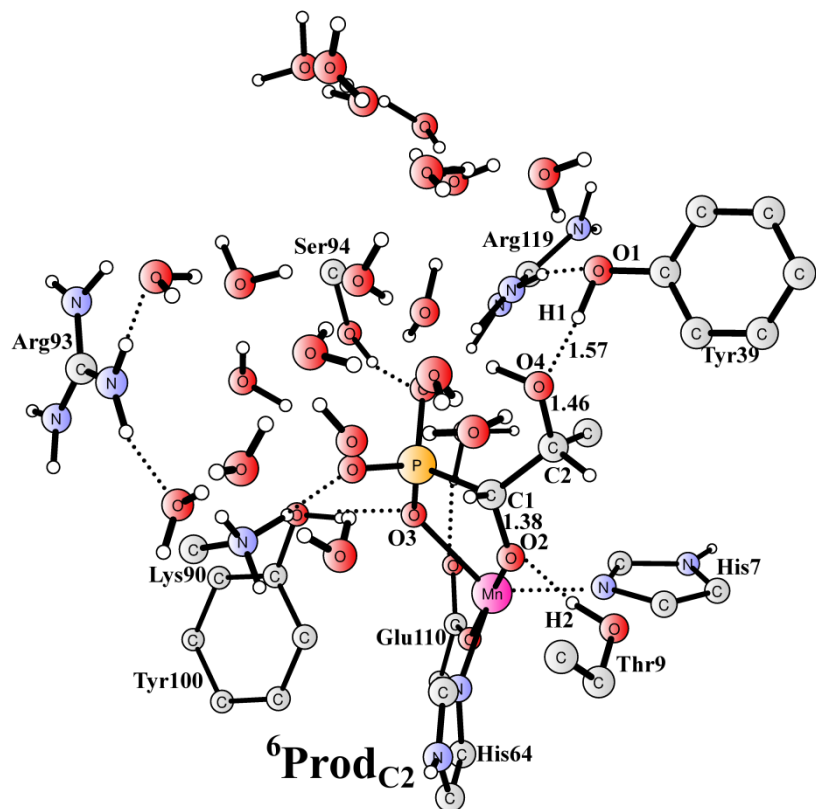
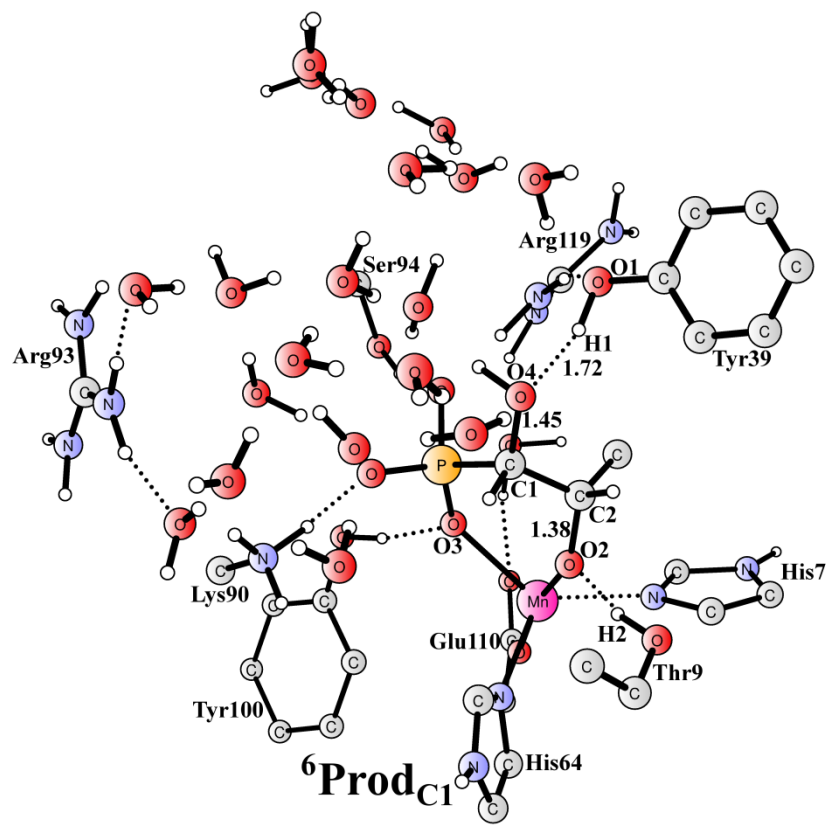


Figure S13. Optimized structure of product complexes for the attack on C1 (${}^6\text{Prod}_{\text{C}1}$) and C2 (${}^6\text{Prod}_{\text{C}2}$) for water attack with QM region M2b (B3LYP/MM). For clarity, unimportant hydrogen atoms are not shown. Distances are given in Å.

Table S5. Calculated QM, MM, QM/MM and dispersion energies (in Hartree) of optimized stationary points for water attack using QM region **M2b**.

	B3LYP/BS1:MM			B3LYP/ TZVPP:MM		Dispersion
	QM	MM	QM/MM	QM	QM/MM	
⁶ React	-5585.310834	-156.171157	-5741.481991	-5590.542121	-5746.713278	-0.265069
⁴ React	-5585.252802	-156.171233	-5741.424035	-5590.485315	-5746.656548	-0.268740
² React	-5585.227065	-156.171231	-5741.398296	-5590.459773	-5746.631004	-0.269469
⁶ TS2_{C1}	-5585.284154	-156.164963	-5741.449117	-5590.509472	-5746.674435	-0.269539
⁶ TS2_{C2}	-5585.287930	-156.166776	-5741.454706	-5590.515674	-5746.682450	-0.267947
⁶ Prod_{C1}	-5585.324606	-156.161891	-5741.486497	-5590.548148	-5746.710039	-0.268129
⁶ Prod_{C2}	-5585.330311	-156.165561	-5741.495872	-5590.551843	-5746.717404	-0.267981

5. Complete citations for references 42, 53, and 55.

- (42) Frisch, M. J.; Trucks, G. W.; Schlegel, H. B.; Scuseria, G. E.; Robb, M. A.; Cheeseman, J. R.; Scalmani, G.; Barone, V.; Mennucci, B.; Petersson, G. A.; Nakatsuji, H.; Caricato, M.; Li, X.; Hratchian, H. P.; Izmaylov, A. F.; Bloino, J.; Zheng, G.; Sonnenberg, J. L.; Hada, M.; Ehara, M.; Toyota, K.; Fukuda, R.; Hasegawa, J.; Ishida, M.; Nakajima, T.; Honda, Y.; Kitao, O.; Nakai, H.; Vreven, T.; Montgomery, Jr., J. A.; Peralta, J. E.; Ogliaro, F.; Bearpark, M.; Heyd, J. J.; Brothers, E.; Kudin, K. N.; Staroverov, V. N.; Kobayashi, R.; Normand, J.; Raghavachari, K.; Rendell, A.; Burant, J. C.; Iyengar, S. S.; Tomasi, J.; Cossi, M.; Rega, N.; Millam, N. J.; Klene, M.; Knox, J. E.; Cross, J. B.; Bakken, V.; Adamo, C.; Jaramillo, J.; Gomperts, R.; Stratmann, R. E.; Yazyev, O.; Austin, A. J.; Cammi, R.; Pomelli, C.; Ochterski, J. W.; Martin, R. L.; Morokuma, K.; Zakrzewski, V. G.; Voth, G. A.; Salvador, P.; Dannenberg, J. J.; Dapprich, S.; Daniels, A. D.; Farkas, Ö.; Foresman, J. B.; Ortiz, J. V.; Cioslowski, J.; Fox, D. J. *Gaussian 09, Revision B.01*, Gaussian, Inc., Wallingford CT, **2009**.
- (53) MacKerell, Jr., A. D.; Bashford, D.; Bellott, M.; Dunbrack, Jr., R. L.; Evanseck, J.; Field, M. J.; Fischer, S.; Gao, J.; Guo, H.; Ha, S.; Joseph-MacCarthy, D.; Kuchnir, L.; Kuczera, K.; Lau, F. T. K.; Mattos, C.; Michnick, S.; Ngo, T.; Nguyen, D.T.; Prodhom, B.; Reiher, III, W. E.; Roux, B.; Schlenkrich, M.; Smith, J. C.; Stote, R.; Straub, J.; Watanabe, M.; Wiórkiewicz-Kuczera, J.; Yin, D.; Karplus, M. *J. Phys. Chem. B* **1998**, 102, 3586-3616.
- (55) Sherwood, P.; de Vries, A. H.; Guest, M. F.; Schreckenbach, G.; Catlow, C. R. A.; French, S. A.; Sokol, A. A.; Bromley, S. T.; Thiel, W.; Turner, A. J.; Billeter, S.; Terstegen, F.; Thiel, S.; Kendrick, J.; Rogers, S. C.; Casci, J.; Watson, M.; King, F.; Karlsen, E.; Sjøvoll, M.; Fahmi, A.; Schäfer, A.; Lennartz, C. *J. Mol. Struct. (THEOCHEM)* **2003**, 632, 1-28.